RESEARCH ARTICLES

ESTIMATION OF CHANNEL SINUOSITY FROM PALEOCURRENT DATA: A METHOD USING FRACTAL GEOMETRY

PARTHASARATHI GHOSH

Geological Studies Unit, Indian Statistical Institute, 203, B.T. Road, Calcutta 700 035, India
e-mail: pghosh@www.isical.ac.in

ABSTRACT: In ancient fluvial deposits, exposure limitations seldom allow direct measurement of channel and valley lengths—the requisite parameters for determination of channel sinuosity. However, sinuosity can be indirectly estimated from dispersion of paleocurrent data, because it is observed in modern rivers that the migration paths of ripples and dunes usually follow the local orientation of the thalweg.

A natural channel can be described to be broadly sinuous in plan. A magnified view of any small part of it is also sinuous in shape. This scale independence of shape can be observed at smaller and yet smaller scales. Fractal patterns, which also have this property, are used here to model channel plan form at the scale of bedform migration paths. It is assumed that the sinuosity of a fractal pattern represents the channel sinuosity over a single meander wavelength, and the orientations of the smallest segments of the patterns are considered to represent the bedform migration directions. An attempt has been made in this study to establish a functional relationship between the sinuosity of the patterns and the dispersion (consistency ratio) of its segment orientations. From a number of fractal patterns of different sinuosity values, the following relationship is noted:

ln Sinuosity = 2.49 − 0.0475 Consistency + 0.000234 Consistency^2.

This relationship can be used to estimate, from paleocurrent data, the sinuosity of short stretches of ancient channels whose sinuosity was steady over time, e.g., bank-stabilized (non-migrating) channels. Published data from a number of modern rivers are used to test the equation, and the goodness-of-fit hypothesis cannot be rejected at 5% level of significance.

The lateral growth of a meander generally involves a gradual increase in the sinuosity of the thalweg. A growing natural meander is modeled by grouping together a number of fractal patterns of different sinuosity values. In a group, the pattern having the maximum sinuosity value represents the thalweg at the last stage of growth, while the rest of the patterns represent the thalwegs at intermediate stages of growth. Partial removal of earlier deposits by erosion associated with the growth of meander is taken into account by excluding the parts of the fractal patterns that represent the intermediate growth stages and lie outside final meander loop. The segment orientations from all the patterns in each group are pooled and compared with the maximum sinuosity value. From a number of such groups (of different maximum values of sinuosity) the relation between the consistency ratio and the maximum sinuosity is found to be

ln Sinuosity = 4.2416 − 0.0801 Consistency + 0.0004 Consistency^2.

An empirical test of this equation using data from a single ancient meandering river deposit yields satisfactory results.

INTRODUCTION

The sinuosity of a channel refers to its geometry in plan and provides a measure of the degree to which a channel departs from a straight-line

course. Leopold and Wolman (1957) defined it as the ratio of channel length to valley length. Brice (1964) proposed a slightly different definition of sinuosity (the ratio of the channel length to the length of the meander-belt axis), which takes into account both straight and curved meander-belt axes.

In case of ancient channel deposits, direct measurements of channel lengths and valley lengths are seldom possible because of limited exposures. However, sinuosity can be indirectly estimated from dispersion of paleocurrent directions (cf. Bluck 1971; Ferguson 1977; Le Roux 1992), because it has been observed that ripples and dunes (sensu Ashley 1990) in modern rivers usually migrate subparallel to the local thalweg (Ferguson 1977). Attempts have been made to establish a relationship between the dispersion of bedform orientations and the channel sinuosity either by direct measurements of bedform orientations in modern river tracts (cf. Bluck 1971), or by inference from the plan geometry of river courses (cf. Ferguson 1977, Le Roux 1992). Bluck (1971) could demonstrate only a qualitative relationship between sinuosity and bedform orientations. Ferguson (1977) and Le Roux (1992) assumed that the tangents to the channel segments at different points, as observed in aerial photographs, represent the migration direction of bedforms. In Ferguson's (1977) study, the segments of channels used to represent the migration directions of the bedforms are much longer than the migration paths of ripples and dunes. Complexities of the local water flow paths (at a higher level of magnification) within the channel segments can give rise to a wider variance in bedform orientations (Bluck 1974, 1979) than what has been accounted for by Ferguson (1977). Moreover, the studies of Bluck (1971) and Ferguson (1977) do not account for temporal changes in meander morphologies, and the application of these relationships to ancient deposits is problematic. Le Roux (1992) did account for the temporal changes in morphology by measuring orientations of abandoned scroll bars, swales, and oxbow lakes in a meander belt along with the present channel. This method can estimate the sinuosity of an ancient river at a large scale (air-photo scale) provided that paleocurrent data can be collected over an area as extensive as the meander belt itself. Exposures of a single channel fill usually comprise one or two point-bar deposits; therefore it is difficult to apply Le Roux's methodology in most cases (Olsen 1993).

The geometry of a natural meandering channel is grossly sinuous. Again, any part of the channel, at a higher magnification, can be considered to bear a resemblance to the whole, the likeness continuing with the parts of the parts and so on to infinity (cf. Korvin 1992). In other words, the meandering river plan forms show self-similar geometry for a range of scales.

Fractal geometry describes objects that are self-similar. Therefore the present work utilizes fractal patterns to model the geometry of channel in plan (Fig. 1). These patterns are used to derive a relationship between channel sinuosity and dispersion of paleocurrent data. Sinuosity of the fractal pattern is assumed to represent channel sinuosity, and the orientations of the smallest segments of the pattern are assumed to represent the bedform migration directions. The model is designed to estimate channel sinuosity for a short stretch (over a single meander wavelength). Therefore, the paleocurrent data, which are usually available for a small part of a fluvial deposit in a field exposure, can be used to estimate the local sinuosity of the precursor channel. The model takes into account two important
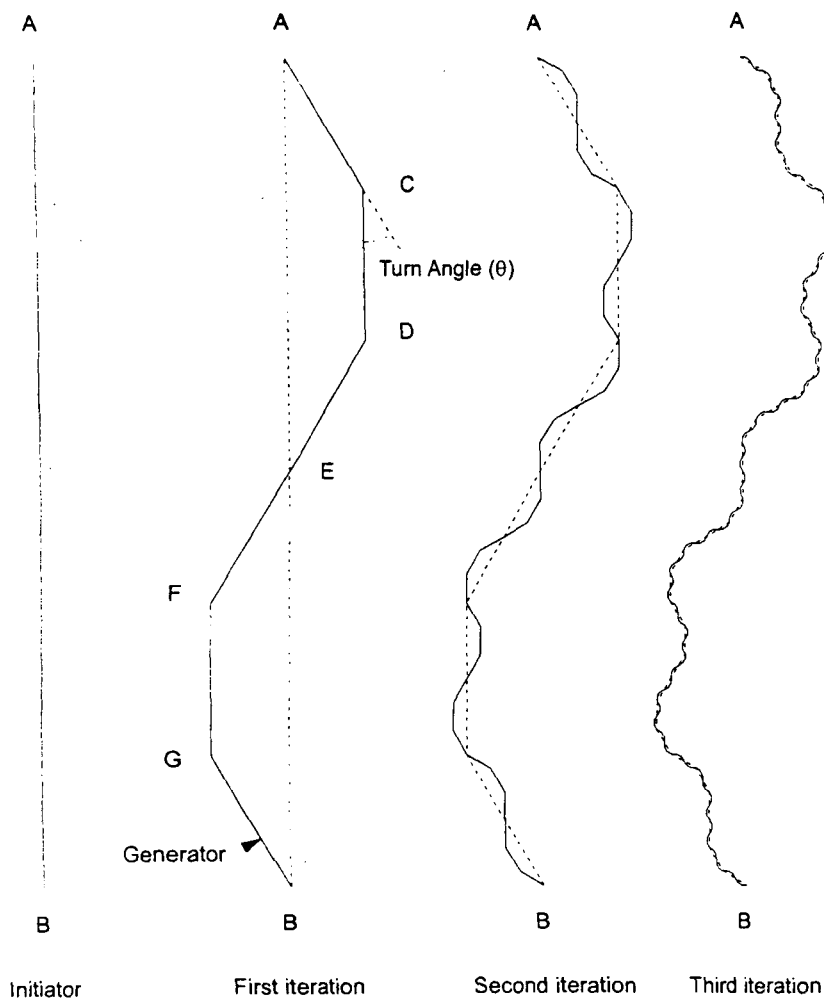
FIG. 1.—Generation of fractal patterns by the L-system technique. In the first iteration. the generator ACDEFGB replaces the initiator AB. In the second iteration. a scaled-down generator replaces each segment of ACDEFGB. The same process is repeated in the third iteration. In each iteration. broken lines show the replaced pattern. In this example. the generator has six segments ($n = 6$) and the turn angle θ is 30°. The sinuosity value of each fractal pattern is calculated by dividing the sum of lengths of all the segments (i.e., the length along the pattern) by the length of line AB. In this example the sinuosity values are 1.10. 1.21. and 1.32 for the patterns obtained after the first. second. and third iterations. respectively.

observations: first. channel length increases with increase in the scale of observations. and second. the planform pattern changes with time, e.g., sinuosity of a meander loop increases with the progradation of the point bar (fig. 5 of Farrell 1987).

The two major parameters used in this study are the channel sinuosity (S) and consistency ratio (L). The channel sinuosity is defined as the thalweg length along two successive identical meanders disposed symmetrically about a straight meander axis/ total axis length of the meanders. The consistency ratio L (Sengupta and Rao 1966) or the "vector magnitude" of Curray (1956) is a concentration measure of orientation vectors and is defined as

$$L = \text{(Magnitude of vector mean/Number of observations)} \times 100$$

The higher values of consistency ratio indicate a strong concentration around the vector mean, whereas lower values indicate a wide dispersion.

METHODOLOGY

An algorithm based upon L-system fractals (Stevens 1993) is used in this study to generate the fractal patterns. The L-system technique begins with an "initiator". which may be a straight-line segment or any geometric figure made up of straight-line segments (Fig. 1). Each side of the initiator is then replaced by a "generator". which is a pattern of straight-line segments of equal length that replaces the original line segment. This process is then repeated in a scaled-down fashion for all the new line segments,

and so forth (Fig. 1). The geometrical shape of the generator is governed by the total number of the segments in the generator (n) and the angle between the adjacent segments (within a quarter of a wavelength), defined as the turn angle (θ). θ and n are constant for all the iterations. so that the shape of the generator is unchanged but for each successive iteration the generator is scaled down such that the endpoints of the generator coincide with the line segment it replaces (Fig. 1).

Range of Channel Sinuosity

A river course at any point of time can have a number of straight stretches and meander loops (figs. 3A and 4A of Alexander et al. 1994). The meander loops can individually expand at different rates. Therefore. though the sinuosity of a long reach of river may remain statistically steady over time. sinuosity (as defined in the context of this study) of a single meander wavelength changes considerably over time (fig. 5 of Farrell 1987). Under the assumptions that meanders are semicircular in plan geometry. disposed symmetrically about the meander axis and growing in unison (Fig. 2, and fig. 1 of Le Roux 1992). Le Roux (1992) showed that the maximum sinuosity of a meander could be 5.24. Beyond that, neck cutoff occurs and the channel ultimately reverts to a low-sinuosity course (Figs. 2, 3). Simultaneous neck cutoff in adjacent meanders produces a channel of sinuosity 1.36 (Fig. 2). Thus. in an idealized situation sinuosity will vary between 1.36 and 5.24. For a natural stream. however. it is very unlikely that the neck cutoff will take place simultaneously. It is more reasonable to assume that the sinuosity of a channel can vary between 5.24 and 1.
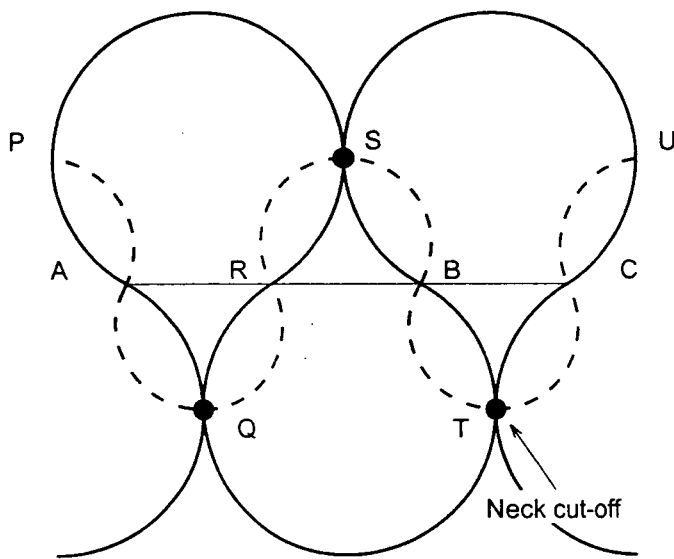
Fig. 2.—Idealized morphology of three adjacent meander loops APSR. RQTB. and BSUC (solid line), where all of them have attained their maximum sinuosity value (5.24) before neck cutoff. ARBC is the meander axis. The broken line represents the probable channel geometry (sinuosity value 1.36) after synchronous neck cutoffs in all the adjacent meander loops.

Fig. 3.—Temporal changes in the morphology of a hypothetical meandering channel.

The Fractal Model

The present work assumes that a straight line, the "initiator" of the fractal pattern, represents the meander axis (Figs. 1, 2). The "generator" approximately takes the shape of a regular sinuous curve (Fig. 1). Three iterations are performed to arrive at the final fractal patterns. In the first iteration the generator replaces the initiator and the resultant pattern is assumed to represent the plan morphology of a large-scale meandering channel (Fig. 1). The second iteration is assumed to incorporate smaller-order variations in the channel orientation. The third iteration is assumed to yield bedform migration directions within the thalweg. Sinuosity is measured as the ratio of length along the pattern (i.e., the product of the length and the total number of the smallest segments of the pattern) to the length of the initiator. Data on segment orientation of the final fractal patterns are presented as rose diagrams using the algorithm of Kutty and Ghosh (1992). The consistency ratios (L) for these orientation data are also calculated (Fig. 4).

To model the plan morphologies of channels, whose sinuosity does not change considerably with time, e.g., the bank-stabilized (nonmigrating) channels, a number of fractal patterns of different sinuosity values (S = 1 to 5.15) are used. Patterns of different sinuosity values are produced by changing the number of segments in the generator from 4 to 36 and keeping the turn angle fixed at 10°.

A point-bar deposit is formed by the growth of meanders. As an individual meander grows, the cut bank shifts and the sinuosity of the thalweg increases from S = 1 to S = S_{MAX} (fig. 5 of Farrell 1987). The shift of the cut bank causes removal of a considerable part of earlier deposits (cf. Hickin 1974 and Farrell 1987). Figure 5 depicts the situation for hypothetical expanding meander loops (some of the channel loci during the meander expansion are denoted by C_1, C_2, ...) (see also fig. 6 in Hickin 1974 and fig. 5 in Farrell 1987). In the examples cited in Figure 5, the laterally migrating channels remove the deposits of the parts of channels represented by dotted lines. The paleocurrent data from these parts will thus be missing in the resulting deposit. The overall effect is a reduction in variance (i.e., increase in consistency ratio) of paleocurrent data in comparison with the precursor bedform orientations in a natural meander.

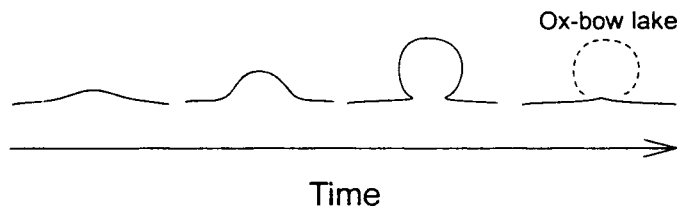A growing natural meander is modeled by a number of fractal patterns

of different sinuosity values grouped together. In a group, the pattern having the maximum sinuosity value, S_{MAX}, represents the thalweg at the last stage of growth, while the rest of the patterns (1 ≤ S < S_{MAX}) represent the thalwegs at intermediate stages of growth. In order to find a suitable method of approximation of the partial removal of earlier deposits due to erosion, half of the wavelengths of all the fractal patterns (in a group) generated after the first iteration are superimposed one upon the other. It is noted that the pattern corresponding to S_{MAX} excludes parts of the extremities of each of the lower-sinuosity patterns. At each extremity, the extent of exclusion ranges from a fraction of a segment to about a pair of segments. For the sake of simplicity it is assumed that the exclusion is uniform in all the intermediate patterns. It is approximated by removing one segment from each end in half-wavelengths (after the first iteration) of all the fractal patterns in a group excepting for the pattern where S = S_{MAX}. Then the second and third iterations are carried out. The segment orientations from all the patterns in each group are pooled and compared with the maximum sinuosity value. Different data sets are generated for S_{MAX} varying between 1.05 and 5.15 (Fig. 4).

RESULTS

A regression analysis between different sinuosity values and their respective consistency ratios suggests (Fig. 6):

$$\ln S = 2.49 - 0.0475L + 0.000234L^2 \tag{1}$$

The following relation has been obtained from the pooled orientation data between S_{MAX} and L (Fig. 6):

$$\ln S_{MAX} = 3.68 - 0.0684L + 0.00032L^2 \tag{2}$$

Test of the Suggested Methodology

Purkait (1983, 1985) studied in detail the bedform orientations on five point bars in the Usri river and one point bar in the Pathri river of Bihar, India, along with the water flow directions in the adjacent thalwegs. To test the validity of the present approach, the water-flow orientation data of Purkait (1983) are used in Eq 1 to estimate the sinuosity values of the thalwegs (Table 1, Fig. 7). Table 1 and Figure 7 show that the estimated sinuosity values are in good agreement with the observed values. However, sample points from the bedform orientation data of Purkait (1983, 1985) are spread all over the surface of the point bar and are not restricted to the thalweg alone. These data represent the orientations of bedforms that migrated during the bank-full discharge and are used to estimate the sinuosity of the centerlines of the rivers between their two banks. Similar bedform orientation data from some other modern rivers (Potter and Pettijohn 1977, Harms et al. 1963, Coleman 1969, Bluck 1971) are also used to estimate the sinuosity of the centerlines of the rivers between their two banks (Table 1, Fig. 7). Some of these studies reported only the standard deviation of the bedform orientations, which are converted to consistency ratios using the relationships suggested by Curray (1956). The estimated sinuosity values again show a correspondence with the observed values (Table 1, Fig. 7). The goodness-of-fit hypothesis for sinuosity values estimated by the
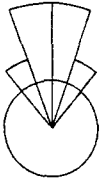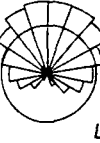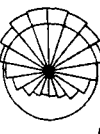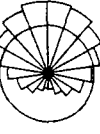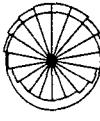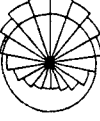
Number of Segments in a wavelength (n)	Sinuosity (S or S_{MAX})	Segment orientations of the individual fractal patterns	Pooled segment orientations for groups of fractal patterns
4	1.05	L=95.54%	L=95.54%
10	1.09	L=91.25%	L=91.5%
20	1.69	L=59.29%	L=70.51%
30	2.48	L=40.38%	L=54.74%
36	5.15	L-19.5%	L=41.85%

Fig. 4.—Rose diagrams showing the dispersions of (i) segment orientations for individual fractal patterns corresponding to the sinuosity values and (ii) pooled segment orientations for groups of patterns corresponding to the maximum sinuosity values. The consistency ratio (L) for each data set is also shown. These data sets are obtained from some of the fractal patterns and some of the groups of patterns used in this study. All the patterns are generated by three iterations, with $\theta = 10°$.

present method is tested using ANOVA model (Table 2). It is noted that the hypothesis cannot be rejected at 5% level of significance.

The test of Eq 2 is rather difficult, because data on both the sinuosity and the bedform orientations from ancient river deposits are scarce. However, the study by Smith (1987) on a well-preserved exhumed Permian point bar from Karoo, South Africa, provides a rare opportunity to verify the utility of Eq 2. The orientation data from the two point bars (where sinuosity can be measured with considerable accuracy) yield a consistency ratio of 63. Using Eq 2 the estimated sinuosity value is 2.19, as compared with the observed sinuosity of 2.22 (Table 1, Fig. 7).

DISCUSSION

The sinuosity of a fractal pattern depends upon the shape of the generator and the number of iterations performed. In the present study, only the number of segments in the generator (n) has been varied to alter the shape of the generator. An alternate method is to keep n constant and let the turn angle (θ) take different values. To compare the two methods, a number of fractal patterns are generated by choosing different combinations of n and θ, (n = 4, 10, ..., 36; θ = 5°, 10°, ... 55°), and S and L are calculated

for each pattern. The scatter diagram of S and L shows that all the points lie on a single curve (Fig. 8). This implies that both of the methods adopted for changing the shape of the generator give rise to the same functional relation between S and L. A fractal pattern generated by low n and high θ can yield S and L values that coincide with S and L values obtained from another fractal pattern generated by high n and low θ. However, for the former pattern (with low n and high θ), the segment orientations show a polymodal distribution (Fig. 9), which is not common in a fluvial setting.

Self-similarity of fractal patterns implies that the length measured along the pattern is directly related to the number of iterations performed, where the length of the initiator is constant. Therefore sinuosity values of fractal patterns increase with increase in the number of iterations (Fig. 1). The scaled-down length, after three iterations, of a single segment of the fractal pattern of lowest sinuosity value as used in this study (n = 4 and θ = 10°) is 0.032 times that of the initiator, whereas that for the fractal pattern of highest value of sinuosity (n = 36 and θ = 10°) is 0.00022 times that of the initiator. This implies that if any of these patterns is used to represent a pair of natural meander loops whose meander axis is 1 km long, the bedform migration paths simulated in this study will range between 32 m
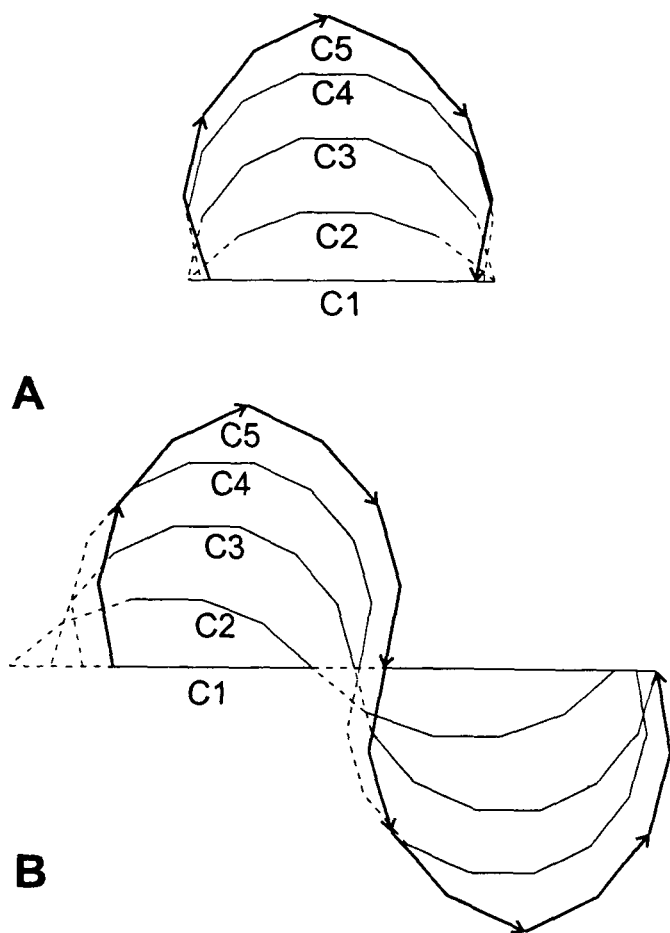
Fig. 5.—Fractal patterns generated after one iteration are superimposed one upon the other to model successive positions of the channels (C1, . . . , C5) in hypothetical expanding meanders. Broken lines represent those parts of the channels where the probable erosion of deposits takes place. The expanding meanders may or may not migrate downvalley as a whole, illustrated by (B) and (A), respectively. In both the situations the dispersions of the segment orientations, likely to be removed due to lateral migration, are similar.

TABLE 1.—*Estimation of channel sinuosity by the suggested method from the published data on bedform and water-flow orientations. The sinuosity values are calculated by using Eq 1 for the data from modern rivers and Eq 2 in the case of paleocurrent data (*).*

Source of Data	Consistency Ratio (L)	Sinuosity (S) Observed	Sinuosity (S) Estimated	Remarks
Twalwegs of different point bars of Usri River. Purkait (1983)	62.3%	1.75	1.55	Water flow directions
	73%	1.5	1.31	
	89.6%	1.18	1.12	
	83.8%	1.2	1.17	
	80.8%	1.38	1.29	
Centreline of Usri River at different point bars. Purkait (1983)	63.4%	1.33	1.42	Bedform orientations on the point bar surface
	74.1%	1.31	1.21	
	71.7%	1.1	1.11	
	81.4%	1.14	1.13	
	70.9%	1.3	1.35	
Centreline of Pathri River. Purkait (1985)	82.2%	1.29	1.18	-do-
Centreline of Vermilion River. Potter and Pettijohn (1977)	74.3%	1.41	1.29	-do-
Centreline of Red River. Harms et al. (1963)	87%	1.11	1.14	-do-
Centreline of Brahmaputra. Coleman (1969)	93%	1.08	1.1	-do-
Centreline of Endrick River. Bluck (1971)	32%	3.36	3.35	-do-
Exhumed Permian point bar (thalweg). Smith (1987)	63%	2.22	2.19*	Paleocurrent data from ancient point bar

and 22 cm. This range is consistent with the lengths of bedform migration paths observed in fluvial settings (figs. 9–10 and 9–11 of Allen 1982: Hamblin 1961; Collinson and Thompson 1989, p. 78). Therefore the patterns obtained after three iterations are considered to be suitable for the present study.

The present work suggests an approximation method, and it should be used in conjunction with a detailed three-dimensional facies analysis and other relevant studies, because knowledge of the details of fluvial depositional history is a prerequisite. The method of estimation of channel sinuosity as outlined here is based on a theoretical model that considers the form of a single channel spanning only a single meander wavelength. Thus the estimates do not indicate the sinuosity of the whole river but instead the local sinuosity of a part of the river for which the paleocurrent data are collected from the exposures. To obtain a meaningful sinuosity estimate using this method, paleocurrent data should be collected from a single channel-fill deposit rather than from a number of adjacent channel-fill bodies. If it is possible to collect paleocurrent data from a single channel-fill body over an extensive length down valley (spanning a number of meander
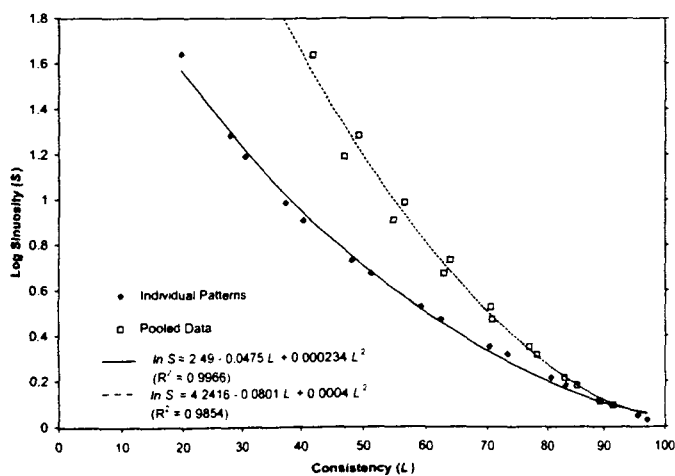

Fig. 6.—Functional relationships between the fractal pattern sinuosity (S) and consistency ratio (L). The solid line represents Eq 1 and the broken line represents Eq 2.
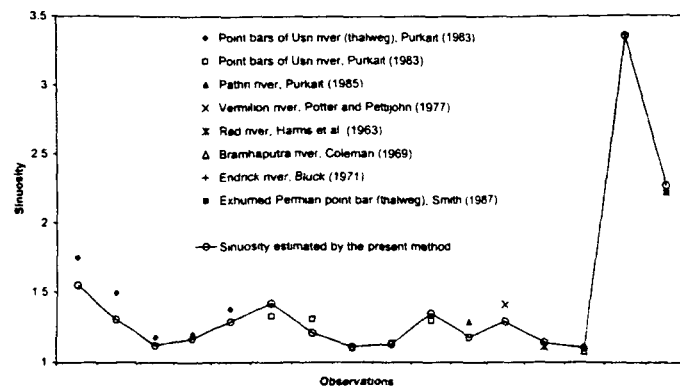

Fig. 7.—A comparison between observed values of sinuosity in modern rivers and that estimated by the present work from published data on bedform and water-flow orientations.
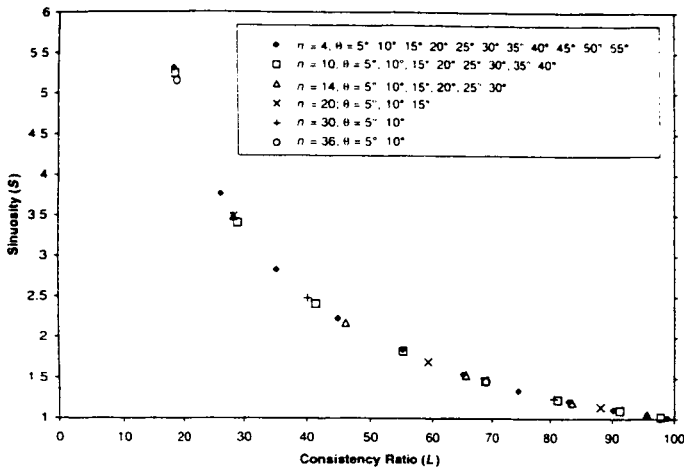
Fig. 8.—Scatter diagram of consistency ratio (*L*) and sinuosity (*S*) obtained from a number of fractal patterns. The patterns are generated by different combinations of *n* and θ (*n* = 4, 10, 14, . . . , 36; θ = 5°, 10°, . . . , 55°). All the data points lie on the same curve, implying that the relation between *S* and *L* does not depend upon the choice of *n* and θ.

wavelengths), an average sinuosity value for the corresponding length of the channel can be estimated.

Orientation data from the flow-parallel primary sedimentary structures like trough cross-strata, rib-and-furrow structure, and parting lineation are suitable for application of the present methodology. In some of the compound cross-stratified sets, foresets are oriented oblique to the flow directions. Orientation data from such features should be avoided, because they can distort the consistency ratio and hence may overestimate the sinuosity.

The change in the shape of channels and their partial erosion related to the growth of point bars is the main theoretical consideration for Eq 2. Therefore, Eq 2 can be used for the point bars only.

CONCLUSIONS

The present work develops a model based on fractal geometry that relates the variability of bedform orientations to the channel sinuosity. This relationship (Eq 1) is tested with published data from a number of modern rivers, yielding satisfactory results. It may also be possible to apply this relationship to estimate the sinuosity of ancient channels if the paleocurrent information from all the parts of a channel thalweg is preserved in the resulting deposit (e.g., the deposits of bank-stabilized nonmigrating channels). However, relocation and modification of the thalweg locus during lateral growth of point bars result in partial removal of earlier thalweg deposits. The relationship between the dispersion of paleocurrent data and

TABLE 2.—*The test of goodness-of-fit hypothesis using ANOVA model between the sinuosity values estimated by the present method and those observed in published natural data from modern rivers.*

	ANOVA Table			
Source	Degrees of Freedom	Sum of Squares	Mean Sum of Squares	F
Model	3	0.8600	0.2867	
Error	12	1.1861	0.0988	2.90
Total	15	2.0461		

the channel sinuosity in such cases would be different from that shown by Eq 1. The present work, considering a simplified model of meander evolution, further derives a relationship (Eq 2) between sinuosity and bedform orientation data for incompletely preserved channel deposits. However, it is expected that in nature the pattern of evolution of natural meanders and the erosion associated with it is likely to be more complex than what has been considered in this work (cf. Stolum 1996, Furbish 1991). The relationship derived in the present work for estimation of sinuosity of ancient channels has been tested successfully with only one natural example. The model appears to have the potential for wide application if it stands further tests with adequate natural data sets and is refined by considering more realistic pattern of meander evolution.

REFERENCES

ALEXANDER, J., BRIDGE, J.S., LEEDER, M.R., COLLIER, R.E., AND GAWTHROPE, R.L., 1994, Holocene meander-belt evolution in an active extensional basin, southwestern Montana: Journal of Sedimentary Research, v. B64, p. 542–559.

ALLEN, J.R.L., 1982, Sedimentary Structures: Their Character and Physical Basis: Developments in Sedimentology, v. 30A, 593 p.

ASHLEY, G.M., 1990, Classification of large-scale subaqueous bedforms: a new look at an old problem: Journal of Sedimentary Petrology, v. 60, p. 160–172.

BLUCK, B.J., 1971, Sedimentation in the meandering River Endrick: Scottish Journal of Geology, v. 7, p. 93–140.

BLUCK, B.J., 1974, Structures and directional properties of some valley sandurs in south Iceland: Sedimentology, v. 21, p. 533–554.

BLUCK, B.J., 1979, Structure of coarse grained braided stream alluvium: Royal Society of Edinburgh, Transactions, v. 70, p. 181–221.

BRICE, J.C., 1964, Channel patterns and terraces of the Loup rivers in Nebraska: U.S. Geological Survey, Professional Paper 422D, p. 1–41.
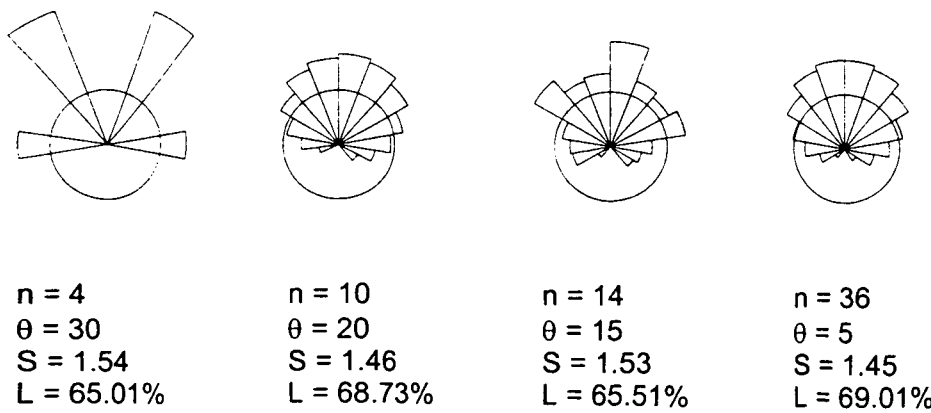

n = 4
θ = 30
S = 1.54
L = 65.01%

n = 10
θ = 20
S = 1.46
L = 68.73%

n = 14
θ = 15
S = 1.53
L = 65.51%

n = 36
θ = 5
S = 1.45
L = 69.01%

Fig. 9.—Rose diagrams representing the dispersions of segment orientations of four fractal patterns generated by different combinations of *n* and θ. Values of *S* and *L* are similar for all the patterns. Note that when *n* is small and θ is large, the rose diagram shows a polymodal distribution.

Coleman. J.M.. 1969. Brahmaputra river: channel processes and sedimentation: Sedimentary Geology. v. 3. p. 129-239.

Collinson. J.D.. and Thompson. D.B.. 1989. Sedimentary Structures: London. Unwin Hyman. 207 p.

Curray. J.R.. 1956. The analysis of two-dimensional orientation data: Journal of Geology. v. 64. p. 117-131.

Farrell. K.M.. 1987. Sedimentology and facies architecture of overbank deposits of the Mississippi river. False river region. Louisiana. in Ethridge. F.G.. Flores. R.M.. and Harvey. M.D.. eds.. Recent Developments in Fluvial Sedimentology: SEPM. Special Publication 39. p. 111-120.

Ferguson. R.I.. 1977. Meander sinuosity and direction variance: Geological Society of America. Bulletin. v. 88. p. 212-214.

Furbish. D.J.. 1991. Spatial autoregressive structure in meander evolution: Geological Society of America. Bulletin. v. 103. p. 1576-1589.

Hamblin. W.K.. 1961. Micro-cross-lamination in Upper Keweenawan sediments of northern Michigan: Journal of Sedimentary Petrology. v. 31. p. 390-401.

Harms. J.C.. Mackenzie. D.B.. and McCubbin. D.G.. 1963. Stratification in modern sands of the Red river. Louisiana: Journal of Geology. v. 71. p. 566-580.

Hickin. E.J.. 1974. The development of meanders in natural river channels: American Journal of Science. v. 274. p. 414-442.

Korvin. G.. 1992. Fractal Models in the Earth Sciences: Amsterdam. Elsevier. 396 p.

Kutty. T.S.. and Ghosh. P.. 1992. ROSE.C—a program in "C" for producing high quality rose diagrams: Computers and Geosciences. v. 18. p. 1195-1211.

Le Roux. J.P.. 1992. Determining the channel sinuosity of ancient fluvial systems from paleocurrent data: Journal of Sedimentary Petrology. v. 62. p. 283-291.

Leopold. L.B.. and Wolman. M.G.. 1957. River channel patterns: braided. meandering and straight: U.S. Geological Survey. Professional Paper 282-B. p. 39-85.

Olsen. T.. 1993. Determining the channel sinuosity of ancient fluvial systems from paleocurrent data—discussion: Journal of Sedimentary Petrology. v. 63. p. 306-307.

Potter. P.E. and Pettijohn. F.J.. 1977. Paleocurrents and Basin Analysis: New York. Springer-Verlag. 425 p.

Purkait. B.. 1983. Current directions in the Usri river point bar. Bihar: Indian Journal of Earth Sciences. v. 10. p. 170-184.

Purkait. B.. 1985. Morphology and growth pattern of the Pathri river point bar. Bihar: Indian Journal of Earth Sciences. v. 11. p. 239-249.

Sengupta. S.. and Rao. J.S.. 1966. Statistical analysis of cross-bedding azimuths from Kamthi Formation around Bheemaram. Pranhita-Godavari valley: Sankhya: Indian Journal of Statistics. Ser. B. v. 28. p. 165-174.

Smith. R.M.H.. 1987. Morphology and depositional history of exhumed Permian point bars in the Southwestern Karoo. South Africa: Journal of Sedimentary Petrology. v. 57. p. 19-29.

Stevens. R.T.. 1993. Advanced Fractal Programming in C: New Delhi. BPB Publications. 305 p.

Stolum. H.H.. 1996. River meandering as a self-organization process: Science. v. 271. p. 1710-1713.